

The dynamics of long wavelength electrostatic turbulence in tokamaks*

D. E. Newman^{†,a)} and P. W. Terry

Department of Physics, University of Wisconsin–Madison, Madison, Wisconsin 53706

P. H. Diamond and Y.-M. Liang^{b)}

Department of Physics, University of California at San Diego, La Jolla, California 92093

G. G. Craddock, A. E. Koniges, and J. A. Crottinger

Lawrence Livermore National Laboratory, Livermore, California 94550

(Received 9 November 1993; accepted 25 January 1994)

From extensive simulation of simple local fluid models of long wavelength drift wave turbulence in tokamaks, it is found that conventional notions concerning directions of cascades, locality and isotropy of spectral transfer, frequencies of fluctuations, and stationarity of saturation do not hold for moderate to long wavelengths ($k\rho_s \ll 1$). In particular, at long wavelengths, where spectral transfer of energy is dominated by the $E \times B$ nonlinearity, energy is carried to short scale (even in two dimensions) in a manner that is anisotropic and highly nonlocal (energy is efficiently passed between modes separated by the entire spectrum range in a correlation time). At short wavelengths, transfer is dominated by the polarization drift nonlinearity. While the standard dual cascade applies in this subrange, it is found that finite spectrum size can produce cascades that are reverse directed (i.e., energy to high k) and are nonconservative in enstrophy and energy similarity ranges (but conservative overall). In regions where both nonlinearities are important, cross-coupling between the nonlinearities gives rise to large nonlinear frequency shifts which profoundly affect the dynamics of saturation by modifying the growth rate and nonlinear transfer rates. These modifications produce a nonstationary saturated state with large amplitude, long period relaxation oscillations in the energy, spectrum shape, and transport rates. Methods of observing these effects are presented.

I. INTRODUCTION

The study of electrostatic plasma turbulence has greatly benefited from simple paradigms that exploit the direct relationship between the physics of collective $E \times B$ motion in plasmas and the turbulent flow of ordinary fluids. This relationship has typically provided the basis for describing saturation of electrostatic instabilities in plasmas. Thus, in a process like that of the inertial cascade of Navier–Stokes turbulence, advective straining by $E \times B$ flow in plasma turbulence is assumed to produce a cascade whose transfer of energy to dissipative scales balances the energy injected by a collective instability. The relationship between $E \times B$ flow and neutral fluid motion has also meant that spectral transfer has generally been assumed to be local (in wave-number space) and isotropic. Transfer in drift wave turbulence in the shorter wavelength part of the spectrum has also been assumed to follow a neutral fluid analogy, namely, two-dimensional (2-D) Navier–Stokes turbulence. For both types of turbulence, a dual cascade is invoked, with energy conservatively cascading to long wavelengths and enstrophy to short wavelengths. Another feature of Navier–Stokes turbulence has also provided a useful analog: the fact that the Kolmogorov spectrum is an energy transfer rate balance under stationary random stir-

ring, thus guaranteeing the stationarity of the saturated state established by self-similar transfer to the dissipation range. By analogy, the driving of collective instabilities in plasmas from fixed gradients maintained by transport balances on the transport time scale has likewise been constructed to lead to stationary saturation.

This paper describes recent studies of the long wavelength drift wave turbulence associated with trapped particle motion in tokamaks that have found that spectral transfer by $E \times B$ advection produces a variety of effects outside the classical phenomenology of cascades in ordinary fluids.^{1–5} These effects include the nonlocality of spectral transfer, anisotropy of transfer, even under isotropic driving and damping, nonconservative cascades by the conservative $E \times B$ advection in spectrum subranges, and the nonstationarity of saturated turbulence. In most cases, these effects ultimately originate from the specific way in which plasma scalar fields, especially the density, are coupled to the flow through the electrostatic potential. In other cases, the presence and nature of sources and sinks, arising from collective instability and dissipation, modify the classical description of cascades, even under transfer processes that are isomorphic to the advective straining of Navier–Stokes turbulence.

These studies examine the spectral transfer and saturation of long wavelength electrostatic fluctuations in tokamaks using a series of simple fluid models with diagnostics designed for investigating the nonlinear dynamics. Four models have been studied in a progression from simple to more complex descriptions. These models consist of

*Paper 417, Bull. Am. Phys. Soc. 38, 1960 (1993).

[†]Invited speaker.

^{a)}Present address: Oak Ridge National Laboratory, Oak Ridge, Tennessee 37831.

^{b)}Present address: Lawrence Berkeley Laboratory, Berkeley, California 94720.

(1) the Hasegawa–Mima equation,⁶ a one-field model of nondissipated drift wave turbulence governed by advective straining of vorticity, a process that dominates spectral transfer at small scales; (2) a one-field description of trapped particle fluctuations^{1,7} spectrally scattered by $E \times B$ advection of the nonadiabatic electron density, a process that dominates at long wavelengths; (3) a one-field model incorporating both of the above processes,⁸ and therefore able to describe spectral transfer under the cross-coupling of the two nonlinearities; and (4) a two-field model governed by the same nonlinear processes, but allowing the nonadiabatic electron density and potential to evolve separately. Permitting separate evolution of nonadiabatic density and potential breaks the artificial constraint that the nonadiabatic density be equal to the potential times a constant multiplier [$\tilde{n}/n_0 = (1 + i\delta)e\phi/T_e$]. This constraint is frequently imposed to achieve a simple one-field description, as in models (1)–(3). In model (4) it is possible for a frequency shift induced by the cross-coupling of the two nonlinearities to affect the stability and dynamics of saturation. Numerical solutions of these models are obtained by spectral techniques, and studied using diagnostics that stress the transfer dynamics and include time histories of total energy and enstrophy, individual mode amplitudes, and power spectra. Particular use is made of a diagnostic that measures spectral transfer rates (as a function of mode number) of energy and enstrophy. With these tools it is possible to investigate the detailed dynamics of the mode evolution and spectral transfer.

II. MODEL PROPERTIES AND BASIC SPECTRAL TRANSFER CHARACTERISTICS

In this section the complete two-field model is briefly presented and some of its main properties are discussed. This is done in the context of comparing and contrasting this model with the one-field reductions of the same system. This analysis examines the linear structure, the integral invariants associated with the two nonlinearities, and the spectral transfer properties of each nonlinearity.

The model utilized for this study is a set of trapped particle fluid equations that couples the dynamics of collisional trapped electrons with hydrodynamic ions through the quasineutrality condition. In previous work based on one-field reductions,^{1,3,4} the inertial response of the electrons was neglected by considering only the most dissipative extreme of collisionality. Here, the electron nonlinearity and inertia terms are included, yielding the model equations:

$$(1 - \sqrt{\epsilon} - \rho_s^2 \nabla^2) \frac{\partial \phi}{\partial t} + V_D \frac{\partial \phi}{\partial y} - \sqrt{\epsilon} V_D (1 + \alpha \eta_e) \frac{\partial \phi}{\partial y} - \sqrt{\epsilon} v_e \tilde{n} + \sqrt{\epsilon} v_e \phi + \rho_s C_s \nabla \phi \times \mathbf{z} \cdot \nabla \rho_s^2 \nabla^2 \phi + \mu \nabla^4 \phi = 0 \quad (1)$$

and

$$\frac{\partial \tilde{n}}{\partial t} + V_D (1 + \alpha \eta_e) \frac{\partial \phi}{\partial y} + v_{\text{eff}} \tilde{n} - C_s \rho_s \nabla \phi \times \mathbf{z} \cdot \nabla \tilde{n} - v_{\text{eff}} \phi = 0, \quad (2)$$

where $\tilde{n} = n_e + \phi$ is the fluctuating electron density plus the fluctuating potential, $V_D = (cT_e/eB)L_n^{-1}$ is the diamagnetic drift velocity, ϵ is the trapped electron fraction, $\eta_e = d \ln T/d \ln n$ is the electron temperature gradient parameter, $v_{\text{eff},e} = v_e/\epsilon$, μ is the coefficient of the hyperviscosity introduced to model strong damping at high k , L_n is the density gradient scale length, $\rho_s = (cT_e/eB)/C_s$ is the ion gyroradius evaluated at the electron temperature, $\alpha = 3/2$, and $C_s = (T_e/m_i)^{1/2}$ is the ion sound speed. The second field \tilde{n} is the total electron density $n_e + \phi$. Evolving this field instead of the nonadiabatic density n_e simplifies the computation. The equation for the nonadiabatic density has a time derivative of ϕ in addition to the time derivative of n_e , making the use of explicit solvers impossible. Advancing the total density also has conceptual advantages: under this description, each field has a single nonlinearity. The $E \times B$ nonlinearity [$\mathbf{v}_E \cdot \nabla \tilde{n}$, where $\mathbf{v}_E = -(c/B_0)\nabla \phi \times \mathbf{z}$ is the $E \times B$ drift] appears solely in the density equation, and the nonlinearity of the polarization drift [arising from $n_0 \nabla \cdot \mathbf{v}_p^{(1)}$, where $\mathbf{v}_p^{(1)} = B_0^{-1}(m_e c/e)\mathbf{z} \times \mathbf{v}_E \cdot \nabla \mathbf{v}_E$ is the advective part of polarization drift] appears solely in the potential equation. These equations reflect the imposition of quasineutrality in order to eliminate the ion density. While the physics of $E \times B$ advection of both electron and ion densities is present in the original equations for electron and ion continuity, the imposition of quasineutrality means that the advection of nonadiabatic electron density governs the $E \times B$ nonlinearity.

The linear dispersion relation for this system is given by

$$(1 - \sqrt{\epsilon} + k^2 \rho_s^2) \omega^2 + [i\nu(1 + k^2 \rho_s^2) - \omega_* (1 - \sqrt{\epsilon} \beta)] \omega - i\omega_* \nu = 0, \quad (3)$$

where $\beta = (1 + \alpha \eta_e)$, $\omega_* = v_D k_y$, and subscripts have been dropped from $v_{\text{eff},e}$. While the exact solution of this quadratic dispersion relation is easily obtained, the properties of the linear instability are more transparent from an iterated solution for $\nu \gg \omega \sim \omega_*$. To lowest order the eigenfrequency is real with $\omega = \omega_*/(1 + k^2 \rho_s^2)$. The second-order frequency is imaginary, yielding the growth rate, $\gamma = -(\omega/\nu)\epsilon^{1/2}[\omega - \omega_* \beta](1 + k^2 \rho_s^2)^{-1}$. For small k , the growth rate goes as k_y^2 , and drops off as k_y^{-2} for large k . In the one-field reduction, these expressions for the frequency and the growth rate appear as constant coefficients multiplying the field amplitude.

It is possible to determine the relative sizes of the $E \times B$ and polarization drift nonlinearities by iterating on Eq. (2) in order to express the factor \tilde{n} in the $E \times B$ nonlinearity in terms of ϕ . For $\nu > \omega$, Eq. (2) yields

$$\tilde{n} = \phi - \frac{v_D}{\nu} (1 + \alpha \eta_e) \frac{\partial \phi}{\partial y}$$

to lowest order. Upon substitution of this expression into the $E \times B$ nonlinearity, $C_s \rho_s \nabla \phi \times \mathbf{z} \cdot \nabla \tilde{n} \rightarrow C_s \rho_s (v_D/\nu) (1 + \alpha \eta_e) \nabla \phi \times \mathbf{z} \cdot \nabla \partial \phi / \partial y$. Comparing the two nonlinearities, it is apparent that the polarization drift nonlinearity dominates the $E \times B$ nonlinearity at very short

wavelengths because it has an additional spatial derivative. At long wavelengths the $E \times B$ nonlinearity dominates. The nominal crossover point is given by the wave number at which the two nonlinearities are equal. This crossover point depends on the effective electron collisionality ν . Assuming rough isotropy, so that $\nabla_{\perp} \approx \partial/\partial y$, this wave number is given by $k\rho_s \approx \delta = C_s/L_n \nu \equiv k_0\rho_s$. The nonlinearities are characterized, not by a single spatial scale, but by a triad interaction consisting of three waves of differing wavelengths. Thus, it is more realistic to identify a region centered about the crossover wave number in which the two nonlinearities are comparable, rather than to speak of a single wave number at which the two are equal. It is within this region that the cross-coupling dynamics are crucial.

With the iterated solution of Eq. (2) substituted into Eq. (1), the turbulent dynamics is described by a single equation with $E \times B$ and polarization drift nonlinearities. Due to the presence of the $E \times B$ nonlinearity, a single quadratic invariant, the energy, is admitted by this system in the absence of driving and damping. From analysis of the statistical mechanics of interacting mode amplitudes in equilibrium, turbulent systems with a single invariant are expected to transfer energy to short wavelengths.^{1,7} This holds provided the stationary spectrum (in a nonequilibrium dynamic state consisting of a cascade-mediated balance between sources and sinks) peaks at long wavelengths or is at worst flat. Transfer to long wavelengths drives enstrophy production,¹ a fact consistent with the breaking of enstrophy invariance by the $E \times B$ nonlinearity. The $E \times B$ nonlinearity is present even in spectral ranges where the polarization drift nonlinearity dominates ($k \gg k_0$). Thus, in a strict sense, enstrophy is not conserved even when the $E \times B$ nonlinearity is weak relative to the polarization drift nonlinearity. However, in such a case, the $E \times B$ nonlinearity accounts for proportionately less of the total energy transfer.³ Because enstrophy production is tied to energy transfer by the $E \times B$ nonlinearity, it can be expected that the importance of enstrophy production in the cascade dynamics diminishes for $k > k_0$. Consequently, transfer in the high- k regime, i.e., transfer dominated by the polarization drift nonlinearity, is consistent with conservation of *both* energy and enstrophy.

A. Short wavelength transfer: The Hasegawa–Mima equation

The above arguments suggest that the enstrophy producing $E \times B$ nonlinearity may be discarded in describing transfer at sufficiently high k . Historically, a one-field system with only the polarization drift nonlinearity, the Hasegawa–Mima equation, was derived by neglecting the nonadiabatic electron density. Without a nonadiabatic electron response, $\bar{n} = \phi$, and the $E \times B$ nonlinearity and instability vanish. Equations (1) and (2) then reduce to

$$(1 - \rho_s^2 \nabla^2) \frac{\partial \phi}{\partial t} + V_D \frac{\partial \phi}{\partial y} + \rho_s C_s \nabla \phi \times \mathbf{z} \cdot \nabla \rho_s^2 \nabla^2 \phi = 0. \quad (4)$$

Because Eq. (4) has two dynamical invariants, a dual cascade is expected on the basis of equilibrium statistical me-

chanics. Enstrophy has two more derivatives than energy and thus tends to concentrate in smaller scales. Accordingly, enstrophy cascades to short wavelengths while the energy undergoes an inverse cascade to long wavelength. This process is identical to the dual cascade of 2-D Navier–Stokes turbulence because the polarization drift nonlinearity is isomorphic to the self-advective nonlinearity of the 2-D Navier–Stokes equation.

The accepted view of the dual cascade holds that from the scale at which energy and enstrophy are externally injected into the system, all of the enstrophy is carried in a self-similar, conservative cascade to short wavelength, and all of the energy is carried self-similarly to long wavelength. In such a cascade there is no improper flow, i.e., no enstrophy is transferred to long wavelength, and no energy is transferred to short wavelength. The validity of this picture was established in a proof that assumed a spectrum of infinite extent and made no allowances for injection at a finite wave number.⁹ Measurements of fluctuations in the core of tokamaks indicate that the spectrum is of very limited extent, encompassing perhaps as little as a decade before dissipation cuts off the transfer.¹⁰ Indeed, an inertial range may not even exist, given the distributed sources and sinks characteristic of collective instabilities in plasmas. However, because spectral transfer is conservative, even in the absence of an inertial range, it is instructive to examine inertial transfer, but in an inertial range that is of limited extent.

The dual cascade of the Hasegawa–Mima equation has been studied numerically and analytically² for a spectrum bounded by wave numbers k_{\min} and k_{\max} into which energy and enstrophy are injected at intermediate wave number k_{inj} . For a finite spectrum extent, it is necessary to account for the energy carried in the conservative enstrophy transfer to short wavelength and the enstrophy carried in the conservative energy transfer to long wavelength. Because a conservative enstrophy cascade carries an invariant amount of enstrophy to smaller scale, the energy associated with those motions must diminish as gradients increase at smaller scale. Similarly, enstrophy carried in the conservative energy cascade must diminish as gradients become smaller at large scale. The nonconserving improper energy cascade that accompanies the usual conservative cascade of enstrophy from k_{inj} to k_{\max} can only be admitted in a conservative system if energy is generated somewhere else in the system in an amount equal to the amount lost in the forward enstrophy cascade. It is possible to recover the net invariance of energy and reduce to the standard dual cascade picture in the limit of an infinite spectrum if a portion of the injected enstrophy cascades conservatively to long wavelength from k_{inj} to k_{\min} . The portion of conservatively cascaded enstrophy carried in the improper direction must be such that the energy generated is equal to the amount of energy lost in the proper enstrophy cascade. Likewise an improper energy cascade must occur in order to obtain a net invariance of enstrophy.

From the relationship $\Omega_k = k^2 E_k$ between energy E_k and enstrophy Ω_k in a given scale k , and the constraint of net invariance, it is straightforward to show that

the amount of energy carried in the proper and reverse (improper) self-similar cascades is given by $E_p = (1/2)E \times (1 - I^2)/(1 - R^2)$ and $E_r = (1/2)E (I^2 - R^2)/(1 - R^2)$, where $I = k_{\text{inj}}/k_{\text{max}}$, $R = k_{\text{min}}/k_{\text{max}}$, and E is the total energy injected at k_{inj} . Likewise $\Omega_p = (1/2)\Omega(I^2 - R^2)/I^2(1 - R^2)$ and $\Omega_r = (1/2)\Omega(1 - I^2)R^2/I^2(1 - R^2)$, where $\Omega = k_{\text{inj}}^2 E$ is the total enstrophy injected. Examination of these relationships shows that the amount of energy and enstrophy in the reverse cascades goes to zero when the spectrum becomes infinite. For finite spectra of limited extent the deviation from the conventional dual cascade picture can be marked. For example, for $k_{\text{inj}} \gtrsim 0.7k_{\text{max}}$, the amount of energy cascaded in the reverse direction toward k_{max} exceeds the amount of energy cascaded in the proper direction toward k_{min} .

B. Long wavelength transfer

In the long wavelength regime ($k \ll k_0$), the polarization drift nonlinearity is weak relative to the $E \times B$ nonlinearity. In such a case there is significant enstrophy production on the nonlinear time scale, consistent with a direct cascade of energy from long wavelengths to shorter wavelengths (within $k < k_0$). The long wavelength Kadomtsev-Pogutse equation⁹ models this process:

$$\frac{\partial \tilde{n}}{\partial t} + D \frac{\partial^2 \tilde{n}}{\partial y^2} + \frac{V_D}{2} \frac{\partial \tilde{n}}{\partial y} + \nu_{\text{eff}} \tilde{n} - \frac{4L_n D}{\epsilon^{1/2}} \nabla \frac{\partial \tilde{n}}{\partial y} \times \mathbf{z} \cdot \nabla \tilde{n} = 0, \quad (5)$$

where $D = \epsilon^{1/2} v_D^2 (1 + \alpha \eta_e) / \nu$. This model has been studied in the context of dissipative trapped ion convective cell turbulence,^{1,7} but is also valid for dissipative trapped electron mode turbulence with modifications in the structure of the linear sources and sinks. The direct transfer of energy by the $E \times B$ nonlinearity to short wavelengths can be anticipated solely on the basis of the existence of a single quadratic invariant, a feature in common with three-dimensional Navier-Stokes turbulence. However, the isotropic, self-similar, local cascade (in wave-number space) conventionally invoked for Navier-Stokes turbulence and enshrined in the Kolmogorov spectrum does not provide an accurate picture of transfer by the $E \times B$ nonlinearity. Isotropy, locality, and self-similarity do not apply to the $E \times B$ nonlinearity. This is evident from the form of the nonlinearity itself. Isotropy is broken by the nonadiabatic electron response, leading to the factor $\partial n / \partial y$ in the nonlinearity. Nonlocality can also be anticipated from the symmetry of the three-wave coupling of the nonlinearity. The symmetrized Fourier transform of the $E \times B$ nonlinearity yields $\nabla(\partial n / \partial y) \times \mathbf{z} \cdot \nabla n \rightarrow -i \Sigma(\mathbf{k} \times \mathbf{k}' \cdot \mathbf{z}) [k'_y - (k_y - k'_y)]$. For highly nonlocal transfer from a long wavelength mode \mathbf{k} , $k_y \ll k'_y$, $k_y - k'_y$. The coupling coefficient is proportional to $(2k'_y - k_y) \approx 2k'_y$ and is thus large if the triad spans a large spectrum range in the k_y direction. Note that for triads spanning a large spectrum range in the k_x direction (but not in k_y) there is no intrinsic favoring of nonlocal transfer over local transfer. By way of contrast, the polarization drift nonlinearity yields $\nabla n \times \mathbf{z} \cdot \nabla \nabla^2 n \rightarrow \Sigma(\mathbf{k} \times \mathbf{k}' \cdot \mathbf{z}) [(k_1 - k'_1)^2 - k_1^2]$ for nonlocal triads.

Here, factors proportional to $k_1'^2$ cancel out, $-2k_1 k_1'$ typically vanishes by symmetry, and the remaining factor k_1^2 is small.

The nonlocality and anisotropy of $E \times B$ transfer is strongly evident in the measurement of transfer rates observed in numerical solutions of Eq. (5). Figures 1 and 2 show local and nonlocal rates of energy transfer from and into bands of constant k_x and k_y . For convenience, nonlocal is defined as energy transferred in a triad interaction linking wave numbers separated by at least half of the spectrum extent. Note that nonlocal transfer dominates local transfer for energy exchanged between bands of different k_y , whereas local and nonlocal transfer rates are comparable between bands of different k_x . The existence of nonlocal transfer is not a mere curiosity. Nonlocal transfer flattens the wave-number spectrum,³ allowing shorter wavelength modes to play a significant role in transport. Moreover, the ability to move energy directly across the spectrum in a single correlation time reduces the nonlinear response time of the spectrum.

III. CROSS-COUPLING OF NONLINEARITIES

When the simple one-field models representing transfer in long and short wavelength extremes are combined, the resulting equation allows description of spectral transfer across the spectrum:

$$\frac{\partial \tilde{n}}{\partial t} + D \frac{\partial^2 \tilde{n}}{\partial y^2} + V_D \frac{\partial \tilde{n}}{\partial y} + \nu_i \tilde{n} - L_n D \nabla \frac{\partial \tilde{n}}{\partial y} \times \mathbf{z} \cdot \nabla \tilde{n} + \rho_s C_s \nabla \tilde{n} \times \mathbf{z} \cdot \nabla \rho_s^2 \nabla^2 \tilde{n} + \mu \nabla^4 \tilde{n} = 0, \quad (6)$$

where ν_i models collisional damping at long wavelength. First studied by Terry and Horton,⁸ subsequent analysis of this equation revealed that the large nonlinear shifts observed in the frequency spectrum¹¹ could be traced to the cross-coupling of the two nonlinearities,³ an effect wholly absent in either of the models reviewed in the previous subsections. The origin of this frequency shift is readily apparent in the simplest closures.^{3,4}

A. Cross-coupling frequency shift

When two quadratic nonlinearities govern spectral transfer, any member of a triad coupled by one of the nonlinearities may be driven by a three-wave coupling of the other nonlinearity. In terms of standard closures, this process is reflected in the iteration of the basic equation, Eq. (6), here rewritten as $\partial n_k / \partial t \sim \Sigma_{k'} \chi_{k, k'}^{(E \times B)} n_{k'} n_{k - k'} + \Sigma_{k'} \chi_{k, k'}^{(\text{Pol})} n_{k'} n_{k - k'}$, where the linear terms are omitted for clarity, and $\chi_{k, k'}^{(E \times B)} = (i/2) L_n D(\mathbf{k} \times \mathbf{k}' \cdot \mathbf{z})(2k'_y - k_y)$ and $\chi_{k, k'}^{(\text{Pol})} = (1/2) \rho_s^3 C_s(\mathbf{k} \times \mathbf{k}' \cdot \mathbf{z}) [(k_1 - k'_1)^2 - k_1^2]$. When the mode $n_{k - k'}$ is nonlinearly driven by fluctuations $n_{-k'}$ and n_k , the direct beating with these fluctuations yields a closed expression for n_k . The driven fluctuation $n_{k - k'}$ is coupled to $n_{-k'}$ and n_k through both nonlinearities: $\partial n_{k - k'} / \partial t \sim (\chi_{k - k', -k'}^{(E \times B)} \chi_{k - k', -k'}^{(\text{Pol})}) n_{-k'} n_k$. The inversion of this equation yields $n_{k - k'} = \Delta \omega_{k - k'}^{-1} (\chi_{k - k', -k'}^{(E \times B)} + \chi_{k - k', -k'}^{(\text{Pol})}) n_{-k'} n_k$, where $\Delta \omega_{k - k'}^{-1}$ is the phase decorrelation time. The closure obtained by substituting for $n_{k - k'}$ in

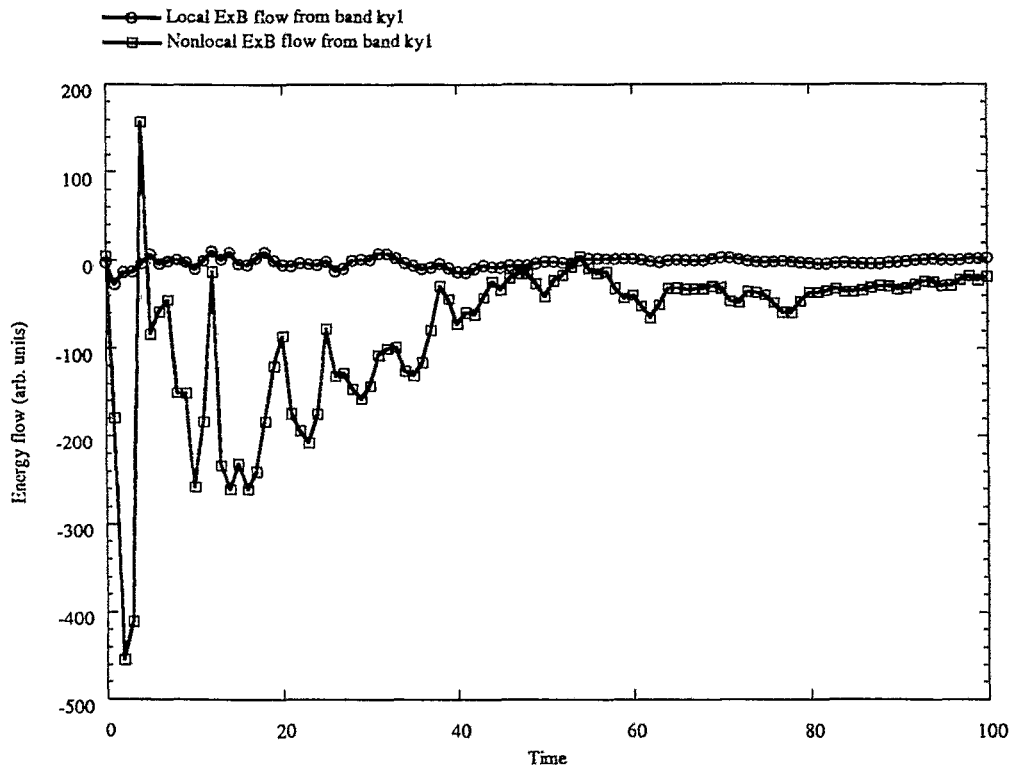


FIG. 1. Local and nonlocal transfer rates from a wave-number band at low k_y .

the expression for $\partial n_k / \partial t$ thus has a product $(\chi_{k,k'}^{(E \times B)} + \chi_{k,k'}^{(Pol)})(\chi_{k-k',-k'}^{(E \times B)} + \chi_{k-k',-k'}^{(Pol)})$. The diagonal self-coupling terms $(\chi_{k,k}^{(E \times B)})^2$ and $(\chi_{k,k}^{(Pol)})^2$ are real and describe loss or increase of energy in the mode n_k by transfer

to other parts of the spectrum. The cross terms $(\chi_{k,k'}^{(E \times B)})(\chi_{k,k'}^{(Pol)})$ are imaginary, a feature rooted in the dissipative nonadiabatic electron response. Assuming the phase decorrelation time $\Delta\omega_{k-k'}^{-1}$ is real, these terms pro-

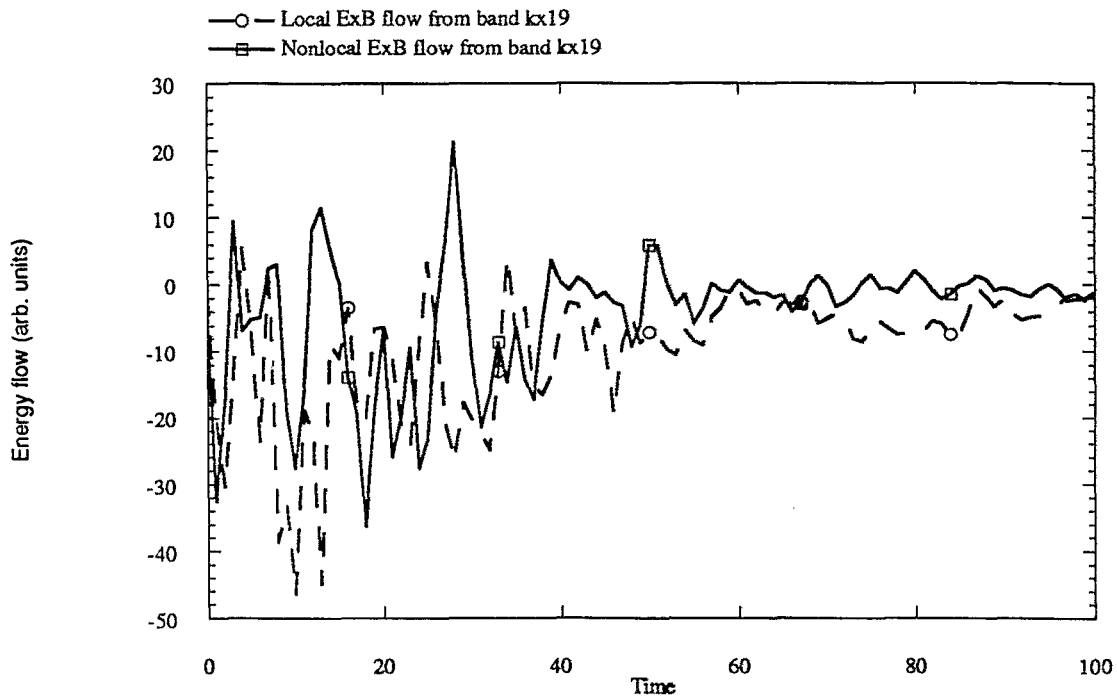


FIG. 2. Local and nonlocal transfer rates from a wave-number band at low k_x .

duce a nonlinear frequency that shifts the eigenfrequency, or peak of the frequency spectrum. Because the phase decorrelation time can, in general, be complex, the cross terms can also contribute directly to the nonlinear transfer rate. For simplicity, if $\Delta\omega_{k-k'}^{-1}$ is treated as real, the frequency shift is given by

$$\begin{aligned} \text{Im } \nu_k &= 2 \sum_{k'} (\chi_{k,k'}^{(E \times B)}) (\chi_{k-k',-k'}^{(\text{Pol})}) \\ &\quad + \chi_{k,k'}^{(\text{Pol})} \chi_{k-k',-k'}^{(E \times B)} |n_{k'}|^2 \Delta\omega_{k-k'}^{-1} \\ &= -L_n D \rho_s^3 C_s \sum_{k'} (\mathbf{k} \times \mathbf{k}' \cdot \mathbf{z})^2 k_y (2k_1^2 - k_1'^2) \\ &\quad \times |n_{k'}|^2 \Delta\omega_{k-k'}^{-1}. \end{aligned} \quad (7)$$

The basic properties of this expression, specifically its amplitude dependence, its dependence on k_y , and the fact that it requires both nonlinearities, have been verified from numerical solutions of Eq. (6).

The cross-coupling contribution to the fluctuation frequency and nonlinear transfer rate significantly modifies spectral transfer in a region around the crossover wave number $k = k_0$. In the immediate proximity of $k = k_0$, the transfer is governed by an amalgam of $E \times B$ transfer, polarization drift transfer and cross-coupling. Moving from k_0 to higher k , $(\chi^{(E \times B)})^2$ quickly becomes subdominant to $(\chi^{(\text{Pol})})^2$. However, because the cross-coupling terms are a geometric mean of $\chi^{(E \times B)}$ and $\chi^{(\text{Pol})}$, they remain significant even after $(\chi^{(E \times B)})^2$ is subdominant. In practice, there is a 1–2 decade span of wave numbers around k_0 in which the cross-coupling frequency shift and transfer rate play a significant role. Beyond this, spectral transfer is governed by either the $E \times B$ nonlinearity (for $k \ll k_0$) or polarization drift nonlinearity (for $k \gg k_0$) as if they existed in isolation. Because the crossover wave number k_0 typically falls within the decade of significant fluctuation power in experimental spectra in tokamaks,¹⁰ cross-coupling effects cannot be ignored in drift wave models.

B. Role of frequency shift on saturated turbulence

In the saturated phase, instability-driven plasma turbulence is usually described in terms of a simple balance between the energy injected by unstable modes and the turbulent spectral transfer to damped fluctuations. Nonlinear frequency effects, such as the cross-coupling frequency shift, are generally ignored since they are oscillatory or reactive, not dissipative. In fact, they can have significant impact on the turbulence levels and transport associated with drift wave fluctuations, because both the growth rate and transport fluxes are proportional to the difference of the fluctuation frequency and the diamagnetic frequency. This difference is usually approximated by using the linear eigenfrequency to represent the fluctuation frequency. In reality, effects such as the cross-coupling frequency shift can strongly modify the linear eigenfrequency at finite amplitude and therefore, the growth rate or rate of energy injection into the turbulence. (It is worth noting that the frequency cannot exceed the diamagnetic frequency. To do

so, the $E \times B$ nonlinearity, which is itself proportional to $\omega - \omega_{*B}$, would have to pass through zero. However, when the $E \times B$ nonlinearity becomes zero, the frequency shift is also zero.¹²) Because the feedback of finite-amplitude-induced frequency shifts on the growth rate of unstable fluctuations requires a frequency-dependent relation between the density and the potential, fixed $i\delta$ models, or first order in time one-field models miss these effects. On the other hand, Eqs. (1) and (2) capture the feedback of the frequency shift on the instability process.

Numerical solutions of Eqs. (1) and (2) indicate that the cross-coupling frequency shift not only modifies the fluctuation levels and amplitude of transport fluxes, but alters the basic temporal behavior of the saturated state. Specifically, the conventional picture of the saturated state as a stationary balance of the phase-averaged spectral transfer and linear growth is no longer valid. Rather, large amplitude, long period oscillations of the total energy, the wave-number spectrum, and the particle flux are observed. The amplitude of these oscillations ranges from 15%–100% of the nominal fluctuation level and the period is of the order of 10 nonlinear interaction (eddy turnover) times. The oscillations are linked to cross-coupling effects because they are not present when the spectrum is arranged so that it lies entirely within either $k \gg k_0$ or $k \ll k_0$. Moreover, the oscillations are strong when $\omega < \nu$ but become weak when $\omega \gtrsim \nu$. When $\omega \gtrsim \nu$, ω replaces $i\nu$ in the nonadiabatic electron response. This changes the complex phase of the $E \times B$ nonlinearity by $\pi/2$ and therefore rotates the frequency shift by $\pi/2$ in the complex plane, making it a contribution to the nonlinear transfer, and no longer allowing it to modify the energy extraction rate. This latter observation is a clue that the amplitude cycles are related to the temporal response of the turbulent saturation to a growth rate that is amplitude dependent through the effect of the frequency shift.¹² It is also observed that variation of the relative strength of the nonlinear transfer rate to the linear growth rate alters both the amplitude and period of the cycles, with the amplitude varying inversely to the period.

The basic cycling phenomenon is illustrated in Fig. 3, which shows the total energy and the energy of a single mode. The rapid fluctuations of the single mode energy indicate the basic nonlinear interaction time scale. This is modulated by a long period envelope corresponding to the cycling. The total energy sums over all modes and largely washes out fluctuations on the nonlinear interaction time scale. Consequently, the long period oscillation in the energy indicates a basic change in the saturation balance. From Figs. 4 and 5, this change is linked to the fluctuation frequency. Figure 4 shows frequency spectra of a mode in the midrange of the wave-number spectrum taken from an ensemble of time histories covering a fraction of a cycle and conditionally triggered near the points of maximum and minimum total energy, e.g., near $t = 10$ and 14 on Fig. 5. The mean frequency $\langle \omega \rangle = \int \omega S(\omega) d\omega$ corresponding to the energy maximum is clearly larger than the mean frequency corresponding to the minimum energy. This is consistent with the amplitude dependence of the cross-

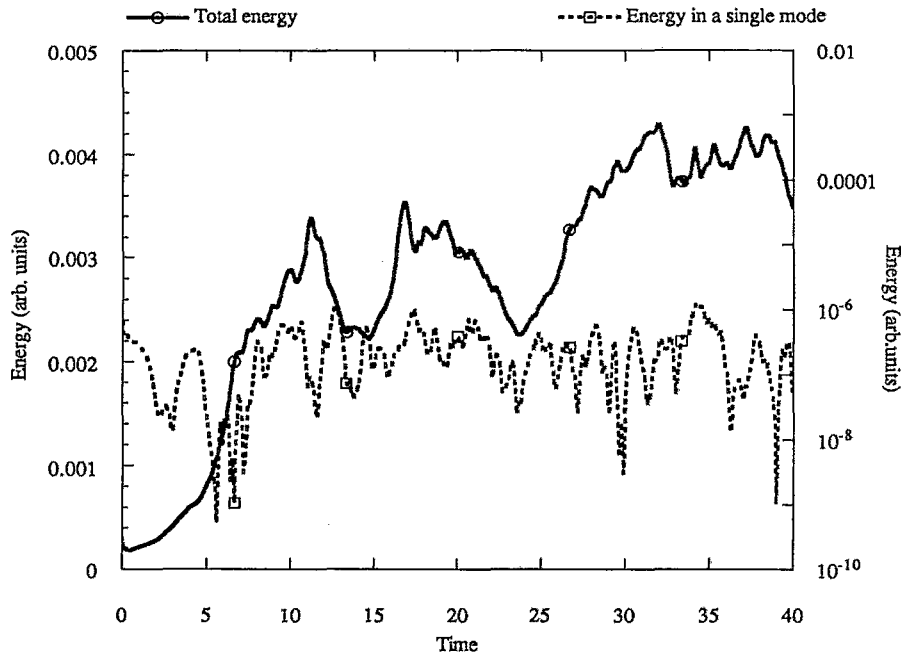


FIG. 3. Total energy and mode energy of an unstable mode. During a cycling event the total energy is seen to fluctuate by more than 15%. The period is 5–10 “eddy turnover times” as defined by a mode fluctuation time.

coupling frequency shift. Because a large frequency shift reduces the growth rate [$\gamma \propto -(\omega - \omega_*\beta)$ with $\omega < \omega_*\beta$], the amplitude collapse is consistent with the growth rate being reduced by the cross-coupling frequency shift.

During a cycling event there is typically bursting in the particle flux. A burst of flux usually leads to the characteristic collapse of energy in the dominant modes. These dominant modes generally lie in the spectrum midrange, near or slightly above the crossover wave number, and are just below the most linearly unstable modes. Near the min-

imum of a cycle, the phase relation between n and ϕ of the low k modes goes to 0. This causes a cessation of transfer from the $E \times B$ nonlinearity, and makes the contribution to the particle flux from these modes become zero (both the flux and the $E \times B$ nonlinearity are maximum when the phase shift between n and ϕ is $\pi/2$, and zero when n and ϕ are in phase). Once the $E \times B$ nonlinearity is zero, the phase is rescrambled by the polarization drift nonlinearity on a nonlinear time scale and the flux and nonlinear transfer resume. From the transfer diagnostic and the wave-

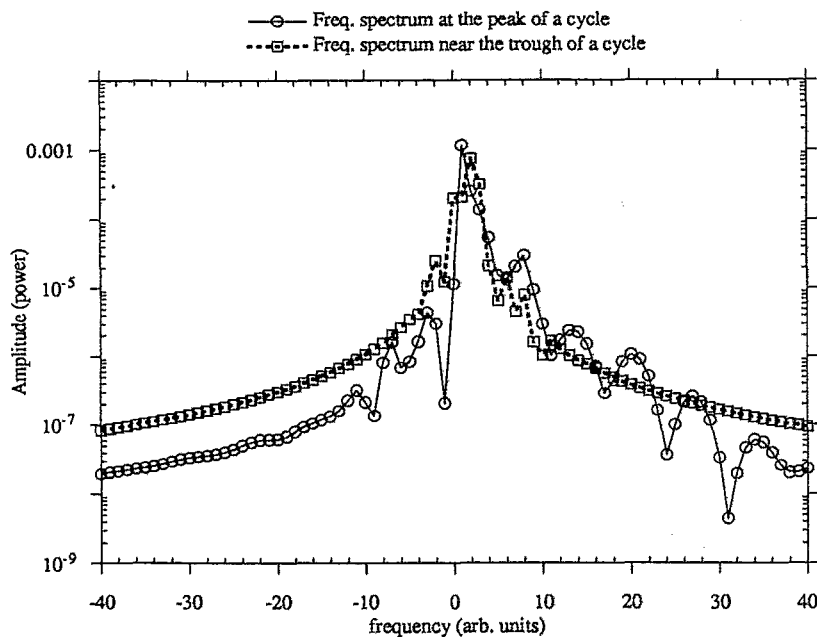


FIG. 4. Frequency spectra from an ensemble of time histories at cycle maxima and minima.

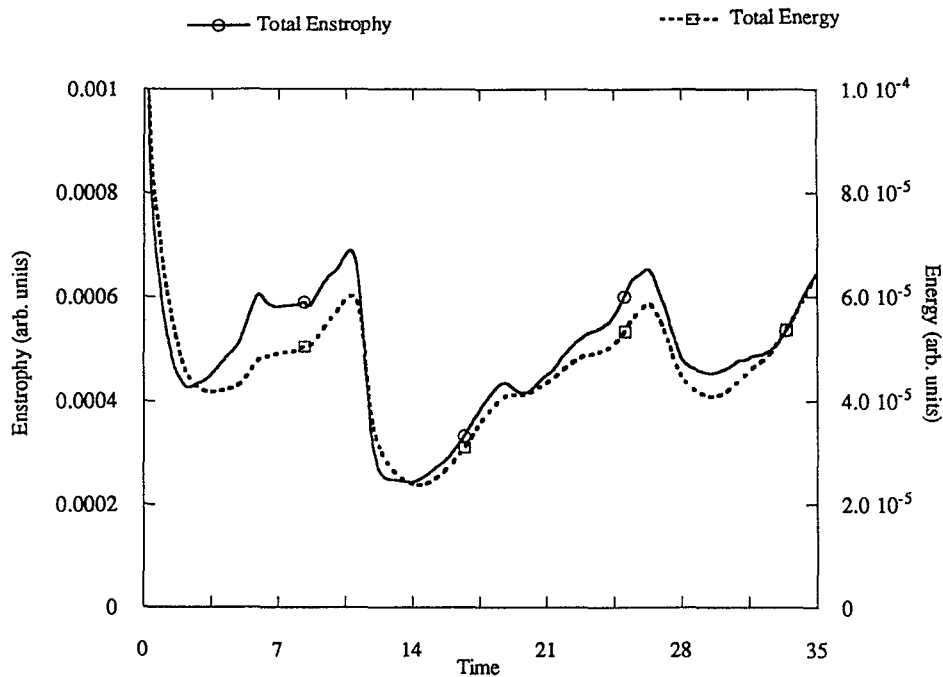


FIG. 5. Energy and enstrophy during several cycles.

number spectrum evolution, the spectrum evolution during a cycle may be described as follows: the most unstable modes increase in amplitude as the energy rises at the beginning of a cycle. Subsequently, a large burst of energy is carried to low k_y , with a smaller amount of energy carried to high k_y . This causes the spectrum to flatten in the k_y direction. As the amplitude collapses, there is a cascade to high k_x attributable to the polarization drift nonlinearity. Simultaneously, the $E \times B$ nonlinearity drives strong transfer to high k . This takes most of the energy to the high- k dissipation region and brings the cycle full circle.

The cycles are also evident in the isodensity contour plots in real space. Structures that are elongated in the x direction appear, grow, and propagate in the y direction, followed by a rapid breakup and subsequent reemergence. This is seen in Fig. 6. The eccentricity of these structures (their x/y dimension) is partially determined by where the crossover wave number k_0 is located relative to the wave number of the most unstable mode. If the most unstable modes are in the $E \times B$ nonlinearity dominated region then the structures are narrower in the y direction due to increased direct, nonlocal transfer to high k_y .

A simple hypothesis for the cause of the cycles can be formulated as follows: at large amplitude, the cross-coupling frequency shift reduces the growth rate, thereby causing the amplitude to fall until the nonlinear transfer has adjusted downward. At lower amplitudes, the frequency shift is smaller and the growth rate becomes larger, forcing the amplitude to rise again. A steady state is impossible because memory effects in the nonlinear response provide the system with finite inertia.

These results indicate that the cross-coupling of nonlinearities produces profound changes in the dynamics of

saturation and behavior of transport. Not only are fluctuation levels modified by the effect of the finite-amplitude-induced frequency shift, but saturation as a stationary phenomenon is no longer possible.

IV. CONCLUSIONS

From simple fluid paradigms for electrostatic fluctuations in tokamaks, it is evident that a variety of simple conventional notions concerning the saturation and spectral transfer of drift wave turbulence must be altered. In particular, the spectral transfer by $E \times B$ advection produces numerous effects outside the classical phenomenology of cascades in ordinary fluids. These effects include (1) the nonlocality and anisotropy of spectral transfer in long wavelength regimes, even under isotropic driving and damping; (2) the existence of nonconservative and reverse cascades in finite spectrum subranges in short wavelength regimes; and (3) the nonstationarity of saturated turbulence due to the cross-coupling of distinct nonlinear coupling processes, specifically the $E \times B$ and polarization drift nonlinearities. The first and third effects originate from the $E \times B$ nonlinearity and the way in which it depends on the relationship between the potential and the nonadiabatic electron density. In the second case, the presence and nature of sources and sinks, arising from collective instability and dissipation, modify the classical description of cascades, even under transfer processes that are isomorphic to the advective straining of Navier-Stokes turbulence.

Because these effects occur at the most basic level of description, they ultimately alter most measurable quantities associated with turbulence, including wave-number

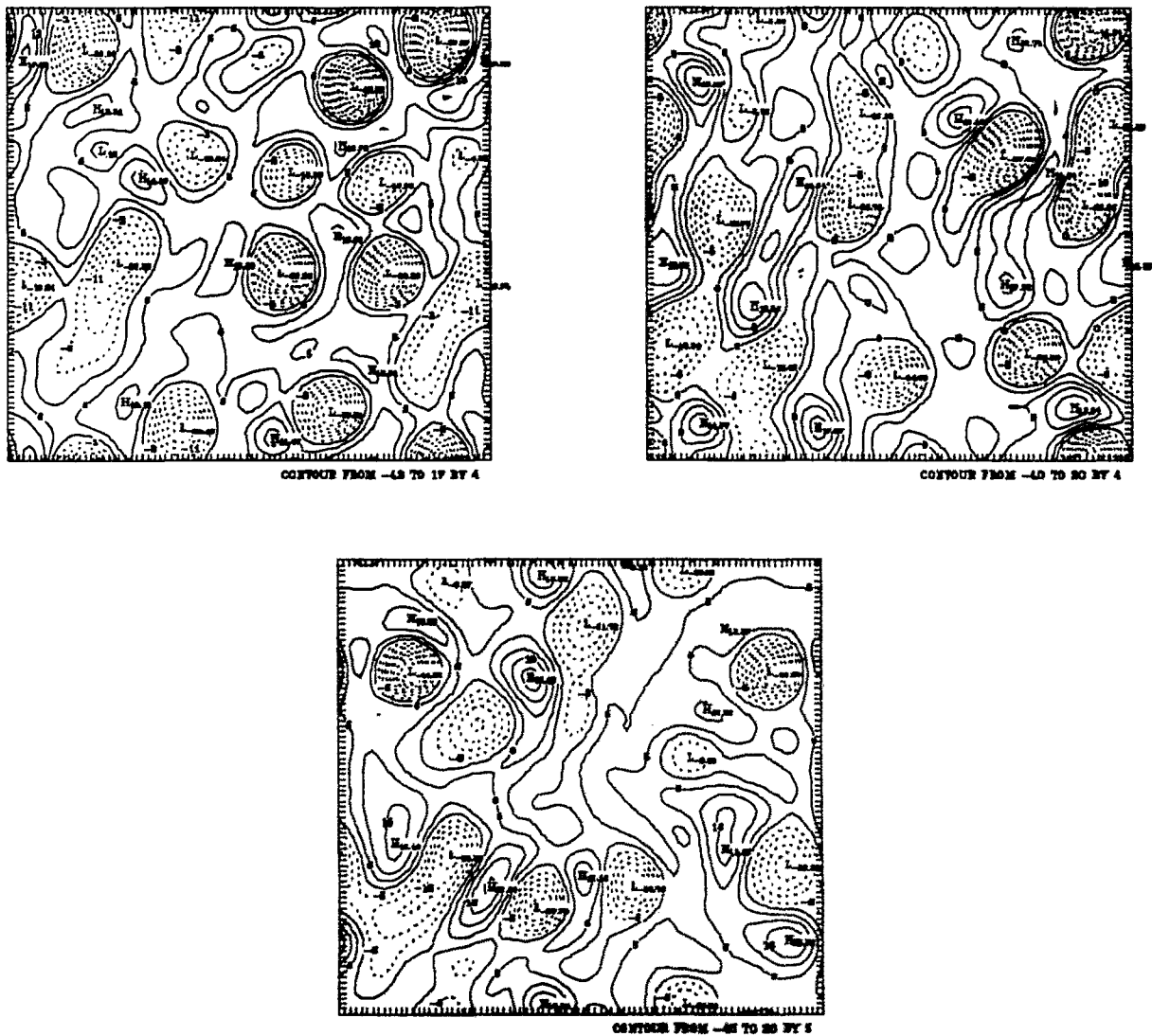


FIG. 6. Real space isodensity contours during a cycle. The structures are relatively isotropic and homogeneous near a cycle minimum. Midway through a cycle they show elongation in the x direction. At the end of a cycle the structures are seen to be breaking up.

and frequency spectra, fluctuation levels, and transport fluxes. Because the models studied herein are inherently simple, it is reasonable to assume that these effects are robust; on the other hand, the specifics of their role under actual experimental conditions may depend on details beyond these simple models.

ACKNOWLEDGMENT

ORNL is managed by Martin Marietta Energy Systems, Inc. under DOE Contract No. DE-AC05-84OR21400 for U.S. D.O.E. This work was supported by U.S. Department of Energy Contract No. DE-FG02-89ER-53291.

¹D. E. Newman, P. W. Terry, and P. H. Diamond, *Phys. Fluids B* **4**, 599 (1992).

²P. W. Terry and D. E. Newman, *Phys. Fluids B* **5**, 2080 (1993).

³D. E. Newman, P. W. Terry, P. H. Diamond, and Y.-M. Liang, *Phys. Fluids B* **5**, 1140 (1993).

⁴Y.-M. Liang, P. H. Diamond, X. H. Wang, D. E. Newman, and P. W. Terry, *Phys. Fluids B* **5**, 1128 (1993).

⁵P. W. Terry, D. E. Newman, H. Biglari, R. Nazikian, P. H. Diamond, V. B. Lebedev, Y.-M. Liang, V. Shapiro, V. Schevchenko, B. A. Carreras, K. Sidikman, L. Garcia, G. G. Craddock, J. A. Crotinger, and A. E. Koniges, in *Plasma Physics and Controlled Nuclear Fusion Research, 1992* (International Atomic Energy Agency, Vienna, 1993), Vol. 2, p. 313.

⁶A. Hasegawa and K. Mima, *Phys. Rev. Lett.* **39**, 205 (1977).

⁷P. H. Diamond and H. Biglari, *Phys. Rev. Lett.* **65**, 2865 (1990).

⁸P. W. Terry and W. Horton, *Phys. Fluids* **25**, 491 (1982).

⁹R. H. Kraichnan, *Phys. Fluids* **10**, 1417 (1967).

¹⁰R. J. Fonck, S. F. Paul, D. R. Roberts, Y. J. Kim, N. Bretz, D. Johnson, R. Nazikian, and G. Taylor, *18th European Conference of Controlled Fusion and Plasma Physics*, Berlin, edited by P. Bachmann and D. C. Robinson (European Physical Society, Geneva, 1991), Vol. 15C, Part I, p. I-269.

¹¹P. W. Terry and W. Horton, *Phys. Fluids* **26**, 106 (1983).

¹²P. W. Terry and P. H. Diamond, *Bull. Am. Phys. Soc.* **38**, 1911 (1993).